Available online at www.sciencedirect.com
ScienceDirect
Ceramics International 37 (2011) 1755–1760
CERAMICS INTERNATIONAL
www.elsevier.com/locate/ceramint

A rapid method for the preparation of silica-coated ZrO_2 nanoparticles by microwave irradiation

Iqbal Ahmed Siddiquey [a,b,d,*], Takeshi Furusawa [a], Masahide Sato [a], Newaz Mohammed Bahadur [c], Md. Nizam Uddin [d], Noboru Suzuki [a]

[a] Department of Advanced Interdisciplinary Sciences, Graduate School of Engineering, Utsunomiya University, Yoto 7-1-2, Utsunomiya 321-8585, Japan
[b] Venture Business Laboratory, Utsunomiya University, Japan
[c] Department of Innovation Systems Engineering, Graduate School of Engineering, Utsunomiya University, Japan
[d] Department of Chemistry, Shahjalal University of Science and Technology, Sylhet-3114, Bangladesh

Received 18 January 2011; received in revised form 25 January 2011; accepted 25 January 2011
Available online 1 February 2011

Abstract

A novel synthesis of silica-coated ZrO_2 nanoparticles is reported based on microwave irradiation (MW) method. The synthesis of silica-coated ZrO_2 nanoparticles was realized by a rapid uniform hydrolysis and subsequent copolymerization of the precursor tetraethoxysilane (TEOS) on ZrO_2 surface. One of the advantages of this MW irradiation method is the very short coating time and uniform heating in comparison to the conventional ones, allowing the synthesis of uniformly coated ZrO_2 nanoparticles with silica. The XPS analysis revealed the shifts in binding energies for Zr 3d5/2 and Zr 3d3/2 peaks after coating confirming the formation of silica layer on the surface of ZrO_2 nanoparticles. Characteristic silica peaks were observed in the FTIR spectra of coated nanoparticles. The shift in the isoelectric point measured by dynamic light scattering method was indicator of silica coverage of the ZrO_2 surface. The coatings formed at 70 °C were thin and uniform and extended up to 2 nm from the ZrO_2 surface as confirmed by the HR-TEM images.

Keywords: A. Sol–gel processes; B. Nanocomposites; D. ZrO_2; E. Functional applications

1. Introduction

Zirconium dioxide (ZrO_2) has wide application in many technological fields, such as high performance ceramics [1], catalysts [2] high-temp fuel cells [3], oxygen sensor [4], damage resistant optical coatings [5] and bioceramics such as orthopedic and dental implants [6]. Due to high refractive index (2.1–2.2) and total transparency to visible light, zirconia is a good white pigment, and a good opacifier [7]. ZrO_2 has also attracted attention as a component to prepare composite materials for catalytic applications. In recent years, research has been focused on the composite particles consisting of a core coated with another compound because of the promising technological applications of such system. Coatings are applied for tailoring the surface and interfacial properties of particles and consequently to improve for instance the dispersability, the thermal stability or the magnetic properties [8–10]. Polymer coating on the surface of ZrO_2 nanoparticles has been reported to decrease agglomeration and improve dispersion of ZrO_2 nanoparticles in organic solvent [11]. Silica coating has been applied on zirconia to enhance its bond strength to resins [12]. Depending on the bond strength of the silica layer to zirconia, the bond strength of the veneering ceramic might also be enhanced. Many reports have shown that tribochemical silica coating of restorations effectively increased the bond strength of resin luting materials to zirconia-based ceramics [13]. Recently ZrO_2–Al_2O_3 and Al_2O_3–ZrO_2 core–shell particles were synthesized and used in ceramic composites, i.e. sintered pellets of ceramics consisting of a matrix phase in which a second phase is incorporated. Zirconia–silica composites have been studied extensively as catalytic surfaces [14,15]. Zirconia–silica composite has also shown potential application as chromatographic support materials. Kanno et al. [16]

* Corresponding author at: Department of Chemistry, Shahjalal University of Science and Technology, Sylhet-3114, Bangladesh. Tel.: +88 0821 716123x251.
E-mail address: iqbal_siddiquey@yahoo.com (I.A. Siddiquey).

0272-8842/$36.00
doi:10.1016/j.ceramint.2011.01.003

reported the preparation of ZrO_2–SiO_2 composite by ultrasonic spray pyrolysis from the mixture solution of the $ZrOCl_2$, $8H_2O$ (ZOC), TEOS, C_2H_5OH and H_2O system. The resulting particles were identified as tetragonal zirconia and amorphous silica. Widoniak et al. [17] prepared silica-coated ZrO_2 particles by conventional method developed by Stober. However, the method required 24 h reaction time to complete the silica coating. Silica has also been used to stabilize metastable tetragonal ZrO_2 [18–23].

The utilization of microwave in synthetic chemistry is a fast-growing research area with immense potential [24–27]. Microwave heating is fundamentally different from the conventional one in which thermal energy is delivered to the surface of the material by radiant and/or convection heating that is transferred to the bulk of the material via conduction. In case of MW heating, it is the absorption of microwave energy followed by volumetric heating involving the transfer of electromagnetic energy to thermal energy. Hence, it is possible to achieve rapid and uniform heating of the materials. Although microwave techniques have been used in organic synthesis since 1984, publications reporting this rapid uniform heating method in the preparation of inorganic composite particles are still limited. In this paper, silica-coated ZrO_2 nanoparticles were synthesized through a rapid route by taking advantage of microwave heating.

2. Experimental

2.1. Materials

The nanopowder used was ZrO_2 (Sigma Aldrich) with primary particle size of 15–25 nm and BET surface area of 35–45 m^2/g. Tetraethoxysilane (TEOS: $Si(OC_2H_5)_4$, 95%) and ethanol (96% synthesis grade) were purchased from Kanto Chemical Co. Inc. Japan. Ammonia solution (28% analytical grade) was purchased from Wako Pure Chemicals Ltd., Japan. All other chemicals were of reagent grade and were used without further purification.

2.2. Silica coating procedure

The flow chart of the silica coating method is shown in Fig. 1. The ZrO_2 dispersions were prepared by a typical ball-milling technique (Pulverisette-7, Fritsch GmbH, Germany). Non-coated ZrO_2 powder (2.5 g) was dispersed into 20 mL of ethanol with 73.2 g of zirconia ball (0.5 mm in diameter) as grinding media in a milling pot and then the grinding was carried out for 10 min by rotating the vessel at 370 rpm. A mixture containing the ZrO_2 dispersion, TEOS, solvent, and aq. NH_3 (pH 12) solution was then MW-irradiated in constant mode in a MW apparatus (Shikoku Keisoku SMW 064, 2.5 GHz, maximum power 500 W) containing a built-in magnetic stirrer plate coated with polytetrafluroethylene (PTFE) in the bottom. The temperature of the mixture was set at 70 °C which was controlled by a thermocouple inserted through a hole in the top of the MW apparatus. MW irradiation was carried out for 2 min. Finally the suspensions were centrifuged at 8000 rpm for 10 min and the solvent was discarded. This washing process of centrifugation and redispersion in ethanol was repeated three times. Subsequently, the coated nanoparticles were dried under vacuum at 110 °C for 2 h to remove remaining solvent and to prepare samples for the characterization.

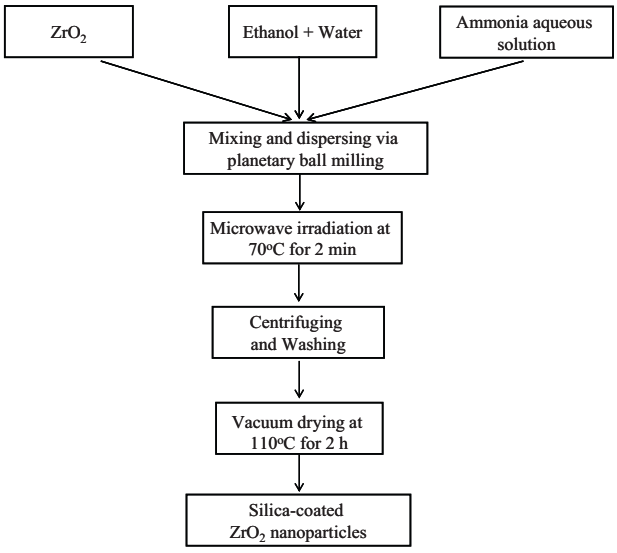

Fig. 1. The flowchart for silica coating of ZrO_2 nanoparticles.

2.3. Surface characterization

The XPS analysis was carried out using a Physical Electronics ESCA-5600 spectrometer with a MgKα X-ray source operating at 200 W (15 Kv to 13 mA). The vacuum in the main chamber was kept above 3×10^{-7} Pa during XPS data acquisitions. The specimens were analyzed at an electron take-off angle of 45°, measured with respect to the surface plane. For all samples, general survey scans (binding energy range: 0–800 eV, pass energy: 187.5 eV) and high resolution spectra (pass energy: 23.50 eV) in the regions of C 1s, Si 2p, O 1s, and Zr 3d were recorded. Binding energies were referenced to the C 1s binding energy at 284.8 eV. The elemental compositions were evaluated by X-ray florescence spectrophotometer (SEA 5120, Seiko) as flat pellet samples. FT-IR spectra were recorded in transmission mode on KBr pellets using a FT/IR-430 spectrometer (Jasco Corp., Japan), collecting 16 scans in the 4000–400 cm^{-1} range with 4 cm^{-1} resolution. BET surface area of the particles was measured using a NOVA 1200e BET surface area and pore size analyzer. Previously adsorbed gases were removed prior to the measurement by outgassing the samples in nitrogen gas at 110 °C for 4 h. Elemental analysis of the coated samples was carried out using Perkin Elmer 2400II (Perkin Elmer, Inc.). To examine the uniformity and the thickness of silica coating, a Hitachi H-7650 high resolution transmission electron microscope was used to obtain HR-TEM micrographs. The zeta potentials of the bare ZrO_2, silica-coated ZrO_2 and SiO_2 particles were measured using the Zeta Plus apparatus (Brookhaven Instr. Corp., USA). The particles (0.02 g) were mixed with 200 mL distilled water and the

mixtures were sonicated for 30 min. The pH values were adjusted by the addition of 0.1 M HCl or NaOH aqueous solution.

3. Results and discussion

The list of samples prepared in this study is shown in Table 1. The precursor TEOS to ZrO_2 weight ratio was varied from 0.1 to 0.5.

ZrO_2 nanoparticles were coated with silica through a controlled hydrolysis reaction of precursor TEOS in the presence of ethanol–water solvent and catalyst (ammonia). Under basic conditions, the hydrolysis of alkoxysilanes proceeds by a nucleophilic mechanism where water dissociates to produce nucleophilic hydroxyl anions (OH^-) in a rapid first step, and then the nucleophilic attack of an OH^- to the silicon atom by a S_N2-type mechanism. When an alkoxide group (OR) is replaced by a hydroxyl group, the electron density of silicon is reduced, accelerating the hydrolysis rate of other alkoxide groups (inductive factors). Once an alkoxide group is hydrolyzed, the others will be hydrolyzed rapidly, followed by the condensation of $Si(OH)_4$ with the hydroxyl groups attached to the surface of the ZrO_2 particles, resulting in the formation of monodisperse silica shells [28,29]. The chemical reactions describing the hydrolysis and condensation of alkoxysilanes invoking the formation of monodisperse silica shells can be briefly written as follows:

$$Si(OR)_4 + 4H_2O \rightarrow Si(OH)_4 + 4ROH$$

$$nSi(OH)_4 \rightarrow nSiO_2 + 2nH_2O$$

Fourier transform infrared (FT-IR) spectroscopy was carried out on bare and silica-coated ZrO_2 nanoparticles (Fig. 2). A broad absorption peak between 3200 and 3700 cm^{-1}, which is assigned to O–H, was detected on both non-coated and silica-coated ZrO_2 nanoparticles. The band at 1630 cm^{-1} corresponds to HOH bending of physically adsorbed water. All silica-coated samples exhibit broad band between 1020 cm^{-1} and 1200 cm^{-1}, which is assigned to the Si–O–Si asymmetric bond stretching vibration [30]. Band at around 967 cm^{-1} can be assigned to stretching vibration modes Zr–O–Si groups in silica-coated ZrO_2 nanoparticles [31]. All of these features indicate the formation of heterogeneous Si–O–Zr bonds at the interface of SiO_2–ZrO_2 prepared in this work.

In order to confirm that the precursor tetraethoxysilane is completely hydrolysed and condensed as SiO_2, the carbon content of the non-coated and silica-coated ZrO_2 nanoparticles were determined by CHN elemental analysis and the results are presented in Table 1. The presence of unhydrolyzed ethoxysilyl group (Si–OEt) is partially responsible for the porous nature of the coating that is often observed in the sol–gel process. From the results, it can be seen that the non-coated ZrO_2 nanoparticles contain 0.1% carbon. The silica-coated samples have slightly higher carbon content than the non-coated sample. The excess carbon could be attributed to the contamination and solvent ethanol, which remains on the surface of nanoparticles even after the washing process.

Table 1
Sample names and carbon contents (C%) from CHN elemental analysis.

Sample	$TEOS/ZrO_2$ Starting ratio	CHN elemental analysis; C (%)
Non-coated ZrO_2	–	0.1
ZrO_2-10 wt%	0.1	0.1
ZrO_2-30 wt%	0.3	0.2
ZrO_2-50 wt%	0.5	0.4

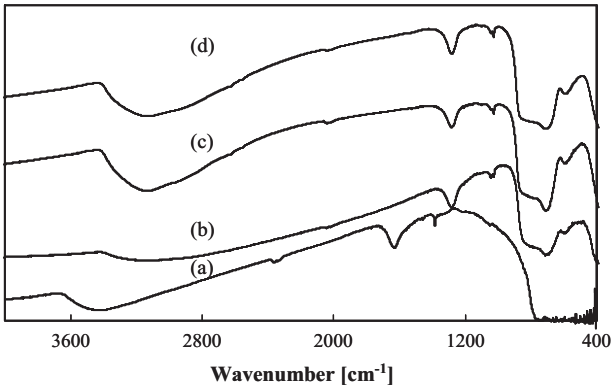

Fig. 2. FT-IR spectra of the (a) non-coated ZrO_2 and silica coated ZrO_2 nanoparticles; (b) Zr-10 wt%, (c) Zr-30 wt%, and (d) Zr-50 wt%.

X-ray photoelectron spectroscopy (XPS) was employed to investigate the surface elemental composition of the bare and silica-coated ZrO_2 nanoparticles. The XPS survey spectra of bare ZrO_2 nanoparticles and silica-coated ZrO_2 particles are shown in Fig. 3. All binding energies were referenced to the binding energy of C 1s at 284.8 eV. The dominant peaks observed for bare ZrO_2 nanoparticles can be assigned to zirconium and oxygen of ZrO_2 nanoparticles. The C 1s peak present in the XPS spectra of non-coated and coated sample because of surface contamination. The XPS spectrum of ZrO_2 after silica coating is similar to that of non-coated ZrO_2 except for the additional Si 2p and Si 2s peaks indicating the presence of SiO_2 on the particles surface.

In order to obtain more detailed information about the nanocomposites, the high resolution spectra of the particular

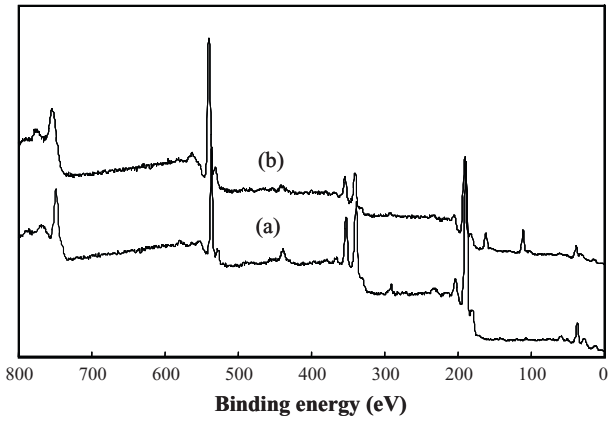

Fig. 3. XPS spectra of the (a) non-coated and (b) silica coated ZrO_2 nanoparticles (Zr-50 wt%).

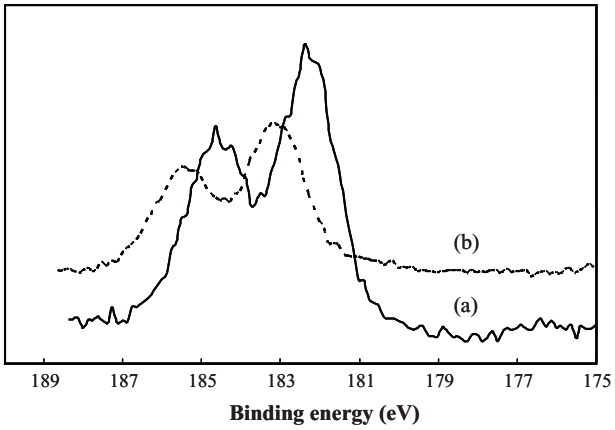

Fig. 4. High-resolution XPS spectra of (a) non-coated ZrO_2 and (b) silica coated ZrO_2 nanoparticles; ZrO_2-50 wt%.

regions were further investigated and shown in Fig. 4. The Zr 3d spectrum for bare ZrO_2 nanoparticles in Fig. 4 shows two doublets of $3d_{3/2}$ and $3d_{5/2}$ which are found at 182.2 and 184.6 eV, respectively. The binding energies and the splitting (energy difference between the $3d_{3/2}$ and $3d_{5/2}$ levels; $\Delta = 2.4$ eV) are in good agreement with the reported values for ZrO_2 particles [32,33].

The binding energy of the Zr $3d_{3/2}$ band (ca. 183.3 eV) in the coated particles was found to be higher than that in ZrO_2 (ca. 182.2 eV), suggesting that the binding energy between zirconium nucleus and inner electrons was changed, and the chemical bond could form between the ZrO_2 cores and the SiO_2 coating component.

The surface atomic concentration of non-coated and silica-coated ZrO_2 particles were determined by XPS and shown in Table 2. The results revealed the presence of the atomic Si, further confirming the successful deposition of silica by the MW assisted method. For bare ZrO_2, the ratio of O to Zr is around 2. From Table 2, the atomic concentration of Si on silica-coated sample (Zr-50 wt%) is 20.8%.

The amount of silica-coated on ZrO_2 particles at different TEOS loadings was characterized by XRF and plotted in Fig. 5. The elemental compositions of the nanoparticles are consistent with the results of the XPS. The Si content increased but the Zr percentage decreased with increasing TEOS loadings. Since larger amount of Si corresponded to thicker silica coating, the data in Fig. 5 indicated that the thickness of silica coating could be easily controlled with TEOS to ZrO_2 weight ratio.

Variations of the zeta potentials (ζ) for bare ZrO_2, silica-coated ZrO_2 particles and SiO_2 particles in aqueous solution are shown in Fig. 6 as a function of pH. The isoelectric point (IEP) is the pH for which the zeta potential is equal to zero. From

Table 2
Elemental composition of samples from XPS analysis.

Sample name	Elemental composition (at.%)			
	C	O	Si	Zr
Non-coated ZrO_2	9.6	60.8	–	29.6
ZrO_2-50 wt%	17.9	54.1	20.8	7.2

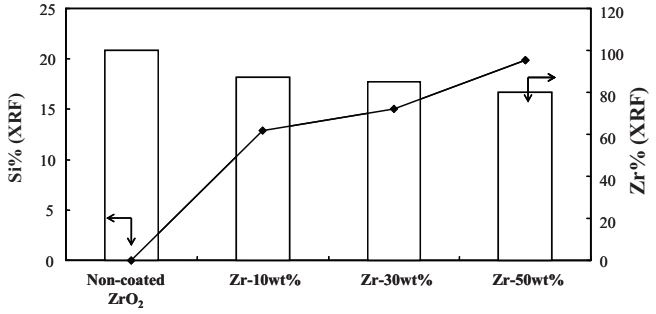

Fig. 5. The elemental composition of Zr and Si on non-coated and silica coated samples from XRF analysis.

Fig. 6, the IEP of ZrO_2 is at about pH 7.4, in the range similar to the data reported in the literature [34,35]. The plot of the zeta potential of the coated particles shows how the coating of a silica layer modifies the zeta potential compared to that of the bare particles. Silica coating reduced the point of zero charge (PZC) of ZrO_2 particles to 2.7 from about 7.4. The IEP has been shifted to low values typical of a silica surface. This result indicates that the silica coating is thick enough to completely mask the underlying zirconia. The dispersion stability of the particles was characterized with the zeta potential value. The particles dispersion is stable when absolute value of zeta potential is above 30 mV [36]. The absolute value of zeta potential was 12 mV at pH 7 for bare ZrO_2 particles. The absolute zeta potential value for silica-coated ZrO_2 nanoparticles was 32.5 mV at pH 7 which is greater than that of bare ZrO_2 nanoparticles. This indicated that repulsion forces between the particles become stronger in silica-coated ZrO_2 particles than the bare ZrO_2 nanoparticles. The coated particles were therefore well dispersed in aqueous solution.

HR-TEM images of the silica-coated ZrO_2 nanoparticles synthesized at TEOS to ZrO_2 weight based ratio of 0.5 are shown in Fig. 7. Because elements with high Z numbers are darker in HR TEM images, the zirconia core and silica shell can easily be distinguished. Darker and lighter parts of particles correspond to zirconia and silica, respectively. HR-TEM analysis revealed that the silica-coated ZrO_2 nanoparticles contain very fine aggregates and large spherical single particles.

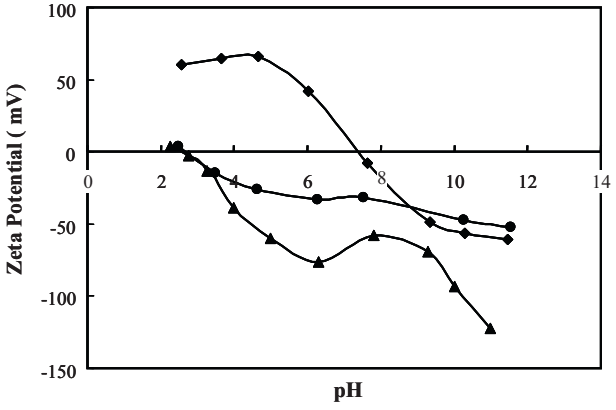

Fig. 6. Variation of zeta potential with pH for bare ZrO_2 (◆), silica coated ZrO_2 (●) and SiO_2 (▲) particles.

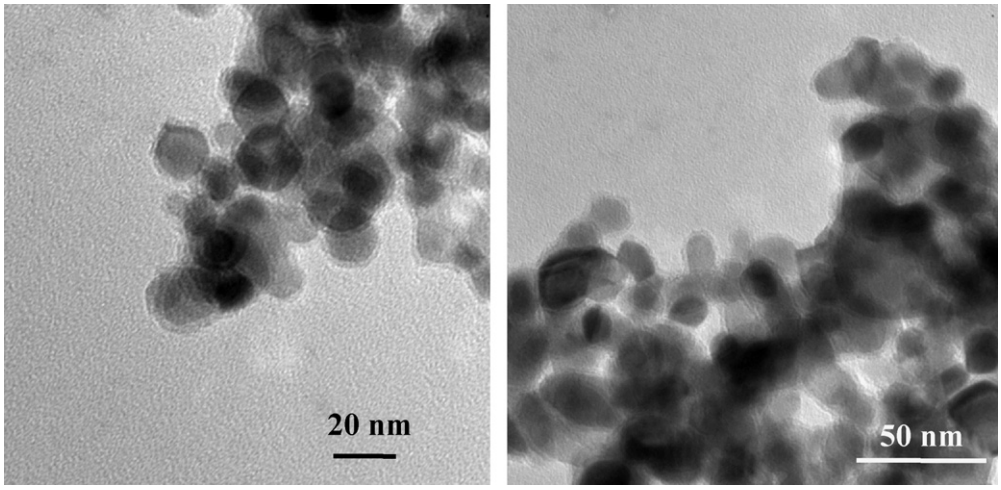

Fig. 7. HR-TEM images of silica coated ZrO_2 nanoparticles.

The core ZrO_2 particles are spherical in shape and ranging in diameter from 15 to 20 nm. There is a uniform continuous shell of SiO_2 with thickness about 2 nm coated on the core of ZrO_2 particle.

4. Conclusions

In this work, the formation of uniform and continuous coating layer of silica on ZrO_2 nanoparticles via the hydrolysis and condensation of the precursor TEOS under a simple and fast MW irradiation method is reported. The analyses of FT-IR, XPS and HRTEM indicate that the composite particles have core–shell structure which is combined through chemical bond of Zr–O–Si. The zeta potential results showed a better dispersion stability of ZrO_2 particles after coating with silica.

Acknowledgement

The financial support from the Venture Business Laboratory (VBL) of Utsunomiya University is greatly appreciated.

References

[1] R.C. Garvie, R.H. Hannink, R.T. Pascoe, Ceram. Steel, Nature 258 (1975) 703–704.
[2] J.F. Haw, J. Zhang, K. Shimizu, T.N. Venkatraman, D.P. Luigi, W. Song, D.H. Barich, J.B. Nicholas, NMR and theoretical study of acidity probes on sulfated zirconia catalysts, J. Am. Chem. Soc. 122 (2000) 12561–12570.
[3] S.P.S. Badwal, Yttria tetragonal zirconia polycrystalline electrolytes for solid state electrochemical cells, Appl. Phys. A 50 (1990) 449–462.
[4] C. León, M.L. Lucı?a, Santamarı?a, Correlated ion hopping in single-crystal yttria-stabilized zirconia, J. Phys. Rev. B 55 (1997) 882–887.
[5] N. Mansour, K. Mansour, E.W.V. Stryland, M.J. Soileau, Diffusion of color centers generated by two photon absorption at 532 nm in cubic zirconia, J. Appl. Phys. 67 (1990) 1475–1477.
[6] J. Li, G.W. Hastings, Oxide Bioceramics: Inert Ceramic Materials in Medicine and Dentistry, Chapman & Hall, London, New York, 1998, p. 340.
[7] P.A. Lewis, Pigment Handbook, vol. I, Wiley, New York, 1988, p. 67.
[8] J.-X. Zhang, L.Q. Gao, Nanocomposite powders from coating with heterogeneous nucleation processing, Ceram. Int. 27 (2001) 143–147.
[9] R.C. Plaza, J.D.G. Duran, A. Quirantes, M.J. Ariza, A.V. Delgado, Surface chemical analysis and electrokinetic properties of sphericalhematite particles coated with yttrium compounds, J. Colloid Interface Sci. 194 (1997) 398–407.
[10] Z. Yu, G. Wu, D. Sun, L. Jiang, Coating of Y_2O_3 additive on Al_2O_3 powder and its effect on the wetting behaviour in the system Al_2O_3p/Al, Mater. Lett. 57 (2003) 3111–3116.
[11] W. He, Z. Guo, Y. Pua, L. Yan, W. Si, Polymer coating on the surface of zirconia nanoparticles by inductively coupled plasma polymerization, Appl. Phys. Lett. 85 (69) (2004) 896–898.
[12] H. Lüthy, O. Loeffel, C.H.F. Hammerle, Effect of thermocycling on bond strength of luting cements to zirconia ceramic, Dent. Mater. 22 (2006) 195–200.
[13] T.T. Heikkinen, L.V. Lassila, J.P. Matinlinna, P.K. Vallittu, Effect of operating air pressure on tribochemical silica coating, Acta Odontol. Scand. 65 (2007) 241–248.
[14] D.R. Acosta, O. Navaro, T. López, R. Gómez, Crystalline phases of sol–gel ZrO_2 in the ZrO_2–SiO_2 system: differential thermal analysis and electron microscopy studies, J. Mater. Res. 10 (6) (1995) 1397–1402.
[15] J.A. Navio, M. Macias, G. Colón, P.J. Sánchez-Soto, Surface characterization of ZrO_2–SiO_2 systems prepared by a sol–gel method, Appl. Surf. Sci. 70–71 (1993) 226–229.
[16] Y. Kanno, T. Suzuki, Estimation of formation mechanism of spherical fine ZrO_2–SiO_2 particles by ultrasonic spray pyrolysis, J. Mater. Sci. 23 (9) (1988) 3067–3072.
[17] J. Widoniak, S. Eiden-Assmann, G. Maret, Synthesis and characterisation of monodisperse zirconia particles, Eur. J. Inorg. Chem. 15 (2005) 3149–3155.
[18] G. Monros, M.C. Marti, J. Carda, M.A. Tena, P. Escribano, M. Anglada, Effect of hydrolysis time and type of catalyst on the stability of tetragonal zirconia–silica composites synthesized from alkoxides, J. Mater. Sci. 28 (1993) 5852–5862.
[19] R.A. Shalliker, L. Rintoul, G.K. Douglas, S.C. Rusell, A sol–gel preparation of silica coated zirconia microspheres as chromatographic support, materials, J. Mater. Sci. 32 (1997) 2949–2955.
[20] T. Ono, M. Kagawa, Y. Syono, Ultrafine particles of the SiO_2–ZrO_2 prepared by the spray-ICP technique, J. Mater. Sci. 20 (1985) 2483–2487.
[21] S.W. Lee, R.A. Condrate Sr., The infrared and Raman spectra of SiO_2–ZrO_2 glasses prepared by a sol–gel process, J. Mater. Res. 23 (1988) 2951–2959.
[22] V.S. Nagarajan, K.J. Rao, Crystallization studies of ZrO_2–SiO_2 composite gels, J. Mater. Sci. 24 (1989) 2140–2146.
[23] J.B. Miller, S.E. Rankin, E.I. Ko, Strategies in controlling the homogeneity of zirconia–silica aerogels: effect of preparation on textural and catalytic properties, J. Catal. 148 (1994) 673–682.
[24] E.B. Celer, M. Jaroniec, Temperature-programmed microwave-assisted synthesis of SBA-15 ordered mesoporous silica, J. Am. Chem. Soc. 128 (44) (2006) 14408–14414.

[25] M. Tsuji, M. Hashimoto, Y. Nishizawa, M. Kubokawa, T. Tsuji, Microwave-assisted synthesis of metallic nanostructures in solution, Chem. Eur. J. 11 (2) (2005) 440–452.
[26] Y.J. Zhu, W.W. Wang, R.J. Qi, X.L. Hu, Microwave-assisted synthesis of single-crystalline tellurium nanorods and nanowires in ionic liquids, Angew. Chem. Int. Ed. 43 (11) (2004) 1410–1414.
[27] S. Makhluf, R. Dror, Y. Nitzan, Y. Abramovich, R. Jelinek, A. Gedanken, Microwave-assisted synthesis of nanocrystalline MgO and its use as a bacteriocide, Adv. Funct. Mater. 15 (2005) 1708–1715.
[28] J.H. Zhang, P. Zhan, Z.L. Wang, W.Y. Zhang, N.B. Ming, Preparation of monodisperse silica particles with controllable size and shape, J. Mater. Res. 18 (2003) 649–653.
[29] D. Pontoni, T. Narayanan, A.R. Rennie, Time-resolved SAXS study of nucleation and growth of silica colloids, Langmuir 18 (2002) 56–59.
[30] T. Lopez, J. Navarrete, R. Gomez, O. Novaro, F. Gigureas, H. Armendariz, Preparation of sol–gel sulfated ZrO_2–SiO_2 and characterization of its surface acidity, Appl. Catal. A: Gen. 125 (2) (1995) 217–232.
[31] Z. Dang, B.G. Anderson, Y. Amenomiya, B.A. Morrow, Silica-supported zirconia. 1. Characterization by infrared spectroscopy, temperature-programmed desorption, and X-ray diffraction, J. Phys. Chem. 99 (1995) 14437–14443.
[32] M. Alvarez, T. López, J.A. Odriozola, M.A. Centeno, M.I. Domínguez, M. Montes, P. Quintana, D.H. Aguilar, R.D. Gonzalez, 2,4-Dichlorophenoxyacetic acid (2,4-D) photodegradation using an Mn+/ZrO_2 photocatalyst: XPS, UV–vis, XRD characterization, Appl. Catal. B: Environ. 73 (1–2) (2007) 34–41.
[33] D.D. Sarma, C.N.R. Rao, XPES studies of oxides of second- and third-row transition metals including rare earths, J. Electron. Spectrosc. 20 (1980) 25–45.
[34] T. Fengqiu, H. Xiaoxian, Z. Yufeng, G. Jingkun, Effect of dispersants on surface chemical properties of nano-zirconia suspensions, Ceram. Int. 26 (2000) 93–97.
[35] J. Wang, L. Gao, Surface and electrokinetic properties of Y-TZP suspensions stabilized by polyelectrolytes, Ceram. Int. 26 (2000) 187–191.
[36] R.H. Muller, K. Mader, S. Gohla, Solid lipid nanoparticles (SLN) for controlled drug delivery—a review of the state of the art, Eur. J. Pharm. Biopharm. 50 (2000) 161–177.